HHS Public Access

Author manuscript

Anal Chem. Author manuscript; available in PMC 2020 August 11.

Published in final edited form as:

Anal Chem. 2020 June 02; 92(11): 7845–7851. doi:10.1021/acs.analchem.0c01090.

Dual-Readout Sandwich Immunoassay for Device-Free and Highly Sensitive Anthrax Biomarker Detection

Isaac N. Larkin,
International Institute for Nanotechnology and Department of Interdisciplinary Biological Sciences, Northwestern University, Evanston, Illinois 60608, United States

Viswanadham Garimella,
International Institute for Nanotechnology, Northwestern University, Evanston, Illinois 60608, United States

Gokay Yamankurt,
International Institute for Nanotechnology and Department of Interdisciplinary Biological Sciences, Northwestern University, Evanston, Illinois 60608, United States

Alexander W. Scott,
International Institute for Nanotechnology and Department of Biomedical Engineering, Northwestern University, Evanston, Illinois 60608, United States

Hang Xing,
International Institute for Nanotechnology and Department of Chemistry, Northwestern University, Evanston, Illinois 60608, United States

Chad A. Mirkin
International Institute for Nanotechnology and Department of Chemistry, Northwestern University, Evanston, Illinois 60608, United States

Abstract

We report a dual-readout, AuNP-based sandwich immunoassay for the device-free colorimetric and sensitive scanometric detection of disease biomarkers. An AuNP–antibody conjugate serves as a signal transduction and amplification agent by promoting the reduction and deposition of either platinum or gold onto its surface, generating corresponding colorimetric or light scattering (scanometric) signals, respectively. We apply the Pt-based colorimetric readout of this assay to the discovery of a novel monoclonal antibody (mAb) sandwich pair for the detection of an anthrax

Corresponding Authors: Chad A. Mirkin — chadnano@northwestern.edu; **Hang Xing —** hangxing@hnu.edu.cn.

Author Contributions

The manuscript was written by I.N.L., H.X., and C.A.M. Experiments were designed and performed by I.N.L., H.X. Additionally, V.G., G.Y., and A.S. performed early PA$_{83}$ oligomerization and characterization studies. All authors have given approval to the final version of the manuscript.

Complete contact information is available at: https://pubs.acs.org/10.1021/acs.analchem.0c01090

ASSOCIATED CONTENT

Supporting Information

The Supporting Information is available free of charge at https://pubs.acs.org/doi/10.1021/acs.analchem.0c01090.

Optimization of the colorimetric detection conditions, ELISA performed with the sandwich antibody pair, and description of blind serum detection (PDF)

The authors declare no competing financial interest.

protective antigen (PA_{83}). The identified antibody pair detects PA_{83} down to 1 nM in phosphate-buffered saline and 5 nM in human serum, which are physiologically relevant concentrations. Reducing gold rather than platinum onto the mAb–AuNP sandwich enables scanometric detection of subpicomolar PA_{83} concentrations, over 3 orders of magnitude more sensitive than the colorimetric readout.

Graphical Abstract

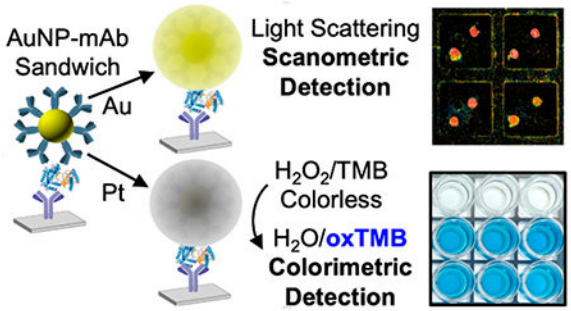

Technologies for the detection of disease biomarkers are key to improving both healthcare and biosecurity around the world.[1] Immunoassays that use antibodies as target recognition elements are the most widely used methods for biomarker detection because of their speed, ease of use, and capacity to detect a wide range of biomarkers and biomolecules.[2] Conventional immunoassays conjugate antibodies to fluorophores or enzymes to convert target binding to detectable fluorescent or colorimetric signals.[3,4] However, these enzymatic fluorogenic and chromogenic methods have well-known drawbacks, including low stability, pH and temperature sensitivity, and limited sensitivity.[5,6]

Over the past 20 years, nanomaterials with tailorable physical properties have been employed in biomarker assays that compare favorably with the molecular fluorophore or enzyme methods on sensitivity.[7–10] A variety of nanoparticle-based readouts, including colorimetric,[11–16] fluorescent,[17–23] light scattering,[24–26] electrochemical,[27,28] and Raman scattering,[29,30] show promise for the development of high-sensitivity detection systems. However, there is a general trade-off between high assay sensitivity and high sample throughput.

For example, anisotropic platinum nanoparticles (PtNPs) and Pt-coated gold nanoparticles (AuNPs) have been deployed in assays as robust, enzyme-free replacements for horseradish peroxidase, where Pt catalyzes the decomposition of H_2O_2 and oxidation of a chromogenic substrate to produce a colorimetric signal.[16,31–33] Such assays require only a few hours of processing time, can analyze many parallel (96–384) samples, and enable device-free visual detection of the target that, in principle, can function in point-of-care or field tests, but their limit of detection is typically confined to the nanomolar to picomolar range.[16,33]

By contrast, scanometric AuNP-based assays have achieved ultrasensitive detection of protein and nucleic acid targets by sandwiching the target between two recognition elements, one immobilized on a glass slide and one attached to the AuNP.[24–26,34,35] Reduction of Ag^+

or Au^{3+} ions from solution onto the AuNPs can amplify the light scattering signal in a laser-scanning instrument to achieve detection of femtomolar to attomolar concentrations of target molecules. However, such assays typically require longer processing times and a specialized scanning instrument; while the glass slides can accommodate a multiplexed analysis of the biomarkers in each sample, the number of samples that can be analyzed in parallel is limited.

The trade-offs between assay field deployability, sample throughput, and assay sensitivity can be reconciled with dual-readout nanoparticle assays, which generate two different types of signal from the same constructs. By combining orthogonal detection methods with different sensitivities, dual-readout assays can lower the limits of detection and quantitation,[36] expand the dynamic range,[37] and enable both high-throughput and ultrasensitive target detection.[35,38]

We present a dual-readout, colorimetric, and scanometric sandwich immunoassay by depositing either Pt or Au onto antibody–AuNP conjugates (Scheme 1). The higher-throughput Pt-based colorimetric readout was used to screen for monoclonal antibody sandwich pairs that bind to anthrax protective antigen (PA_{83}), detecting nanomolar concentrations of PA_{83} in both PBS and human serum. The Au-based scanometric readout showed a 1000-fold increase in assay sensitivity with the same nanoparticles, enabling the detection of subpicomolar PA_{83} concentrations.

EXPERIMENTAL SECTION

Reagents.

Citrate-capped gold nanoparticles (13 and 40 nm) were purchased from Ted Pella or synthesized as previously described.[39] The seven screened anti-PA_{83} antibodies (Ab8240, Ab1988, Ab1990, Ab1991, Ab1992, Ab13808, and Ab38725) were purchased from AbCam. *N*-Hydroxy succinimide (NHS)-activated 96-well plates (divided into 8-well strips), NHS-activated glass slides for scanometric detection, aliquots of Ab1992, and EZ-Link Plus-activated peroxidase kits for horseradish peroxidase-antibody conjugation were purchased from Thermo Fisher. All other materials, buffers, and reagents, including platinum and gold salts, were purchased from Sigma-Aldrich.

Buffered Solutions.

Blocking solution, used for all blocking and washing steps during mAb–AuNP synthesis and PA_{83} detection assays, contained 1× phosphate-buffered saline (PBS), 1% bovine serum albumin (BSA), and 0.02% Tween 20. The platinum deposition solution, used during colorimetric detection, contained 10 mM citrate buffer (pH 3), 20 mM L-ascorbic acid, and 2 mM potassium hexachloroplatinate (K_2PtCl_6). The colorimetric detection solution contained 50 mM H_2O_2 in 3,3′,5,5′-tetra-methylbenzidine (TMB) and was prepared fresh before each colorimetric detection experiment. The gold reduction solution contained 10 mM chloroauric acid ($HAuCl_4$) with 10 mM hydroxylamine (NH_2OH), and was prepared fresh before each gold reduction reaction.

Synthesis of Antibody-Coated Gold Nanoparticles.

Antibodies were noncovalently adsorbed onto the surface of AuNPs, similar to previously described methods.[40] In a 15 or 50 mL plastic conical tube, a solution of 10 nM of citrate-capped AuNPs in water (40 nm diameter for dynamic light scattering (DLS) particle size measurements; 13 nm diameter for all other experiments) was adjusted to pH 7 using 0.2 M NaOH, and Tween 20 was added to a final concentration of 0.02%. Unmodified antibodies were added to a final concentration of 15 μg/mL, and the solution was mixed gently by inverting the tube 4–6 times. The tube was incubated overnight at room temperature in the dark. The mAb–AuNP mixture was then diluted 1:1 with a blocking solution, gently mixed by inverting the tube 4–6 times, sealed by capping the tube and wrapping the cap in parafilm, and incubated for 3 h in the dark at room temperature. The crude mAb–AuNPs were cleaned via two rounds of pelleting (4000 RCF for 30 min at room temperature in 1.5 mL low-retention plastic tubes), supernatant removal, and resuspension in blocking solution. This protocol generates mAh-AuNP nanoparticles that maintain function for at least 3 months at 4 °C.

Characterization of Antibody-Coated Gold Nanoparticles.

The nanoparticle concentration was measured by UV–vis spectroscopy on a Cary5000 spectrophotometer (gold absorption peak at 520 nm, extinction coefficient of 2.7×10^{-8} L/mol/cm). To characterize protein adsorption to the gold surface, particles were twice centrifuged at 4000 RCF for 30 min and resuspended in 1× PBS with 0.02% Tween (no BSA), and then, absorption at 280 nm was measured via UV–vis. To measure the size of mAb-coated AuNPs, mAb–AuNPs were twice centrifuged at 4000 RCF and resuspended in 1× PBS (no BSA or Tween), diluted to 0.5–1 nM AuNP, and measured in a Malvern Zetasizer DLS instrument.

Making Antibody-Coated Wells.

50 μL of 2 mg/mL antibody solution was diluted with an equal volume of 1× PBS (pH 7.5) to make 100 μL of 1 mg/mL antibody solution. Then, 10 μL of the 1 mg/mL antibody solution was carefully and evenly added to the center of each well in a strip of 8 NHS ester modified wells. The strip was incubated overnight in a sealed chamber with a water reservoir (roughly 50% humidity). Then, 100 μL of blocking solution was pipetted into to each well and gently mixed. After 2 min of incubation, the liquid was removed from the strip. These washing steps were repeated twice more. The strips were stored in a humid chamber before use to avoid drying them out. For screening, eight antibody-coated 8-well strips were made, one for each antibody and a BSA control. For further PA_{83} detection assays, mAb 1992 was functionalized on the NHS-activated surface.

Screening for Antibody Sandwich Pairs.

Three mL of the 500 nM PA_{83} solution in 1× PBS and 1 mL of the 1 μM BSA solution in 1× PBS were prepared. To each of the eight 8-well strips, 50 μL of the 500 nM PA_{83} solution was added. The strips were incubated in the humid chamber for 1 h and then washed three times with blocking solution. Next, 50 μL of 10 nM antibody-functionalized nanoparticles was added to each well, such that every combination of immobilized antibody and mAb–

AuNP was tested, along with the BSA negative controls. The strips were incubated in the humid chamber for 1 h and then washed with blocking solution three times. During incubation, a 4 mL batch of a platinum deposition solution, which uses ascorbic acid to reduce Pt(IV) ions onto gold nanoparticles,[33] was prepared from stock solutions. Then, 50 μL of the platinum deposition solution was added to each well. After incubating the strips for 1.5 h in the humid chamber, all wells were gently washed five times with DI water, and 10 mL of a colorimetric detection solution was prepared; 100 μL was added to each well. Strips were incubated in a dark humid chamber for 20 min, avoiding light to minimize background signals. PA_{83} detection was assessed qualitatively by eye, imaged on an Alpha-Innotech FluorChem Q imager, and quantitatively measured via absorbance at 655 nm in a Bio-Tek H4 plate reader.

Colorimetric PA_{83} Detection Curves and Kinetics.

Three 8-well strips were coated with Ab1992, and 5 mL of the AuNPs coated with Ab8240 were prepared, as described above. A dilution series of PA_{83} in 1× PBS was prepared, comprising 1 mL each of 500, 100, 20, 5, 1, 0.5, and 0.1 nM PA_{83} as well as a 1 μM BSA control. 50 μL of each PA_{83} concentration and the BSA control were added in triplicate to the coated 8-well strips. Incubation, washing, addition of mAb–AuNPs, and platinum reduction were performed as described above. Then a colorimetric detection solution was added to all wells. The strips were immediately placed in a Bio-Tek H4 plate reader, and the absorbance at 655 nm was measured every minute for 25 min. The strips were then photographed with an Alpha Innotech FluorChem Q imager under white light.

Serum PA_{83} Detection Curve.

Triplicate Ab1992-functionalized 8-well strips, and a 5 mL batch of Ab8240-functionalized AuNPs were prepared as described above. Human serum solution was prepared by diluting human serum 1:1 in 1× PBS. A dilution series of PA_{83} concentrations (500, 100, 20, 5, 2, 1, and 0.5 nM) was prepared by serially diluting 8 μM stock PA_{83} into a human serum solution. The incubation of PA_{83} dilutions and the control 1 μM BSA in human serum and subsequent colorimetric detection were performed as described above. The absorbance at 655 nm was quantified by plate reader after 20 min of incubation with the colorimetric detection solution.

Scanometric PA_{83} Detection.

200 μL of 1 mg/mL mAb 1992 solution was prepared by diluting antibody stock 1:1 in 1× PBS. NHS-activated glass slides were divided into 10 wells by the attachment of a rubber gasket. Two replicate 5 μL spots of Ab1992 solution were pipetted into each well, and the slide was incubated overnight in the humid chamber. The slide wells were then washed three times with blocking solution. To determine the scanometric detection range of PA_{83}, a dilution series of PA_{83} concentrations (60 nM, 6 nM, 600 pM, 60 pM, 6 pM, and 600 fM) were prepared in 1× PBS and incubated in two replicate wells for 1 h in the humid chamber. The wells were washed 3 times with blocking solution and then incubated for 1 h with 10 nM 8240-modified AuNPs. Wells were washed 3 more times with blocking solution, and then, two gold reductions were performed to amplify the signal.[25]

To perform gold reductions, the slide was removed from the rubber gaskets. Solutions of 10 mM $HAuCl_4$ and 10 mM NH_2OH were prepared in separate 10 mL syringes. The syringes were connected by a T-junction to a single output tube to enable rapid mixing of the solutions. Then, 4 mL of a 1:1 $HAuCl_4/NH_2OH$ mixture was spread evenly over the surface of the slide for 30 s, and then, the slide was immersed in a DI water bath to wash the gold reduction solution away, gently rinsed with running DI water, and blown dry with N_2. The gold reduction, washing, and drying steps were repeated once more. The slide was then imaged with a Tecan LS Reloaded scanner. Light scattering signal intensities from the two replicate spots for each PA_{83} concentration were quantified by GenePix Pro 6 software. The limit of detection was determined using 3.5 sigma above the negative control and fitting the data points to a Hill equation.

RESULTS AND DISCUSSION

Assay Overview.

The dual-readout sandwich immunoassay begins with the immobilization of one set of antibodies (Ab1) via lysine conjugation onto an *N*-hydroxy-succinimidyl-ester (NHS)-modified surface (either in a 96-well plate for colorimetric detection or on a glass slide for scanometric detection). In parallel, we synthesized Ab–AuNP conjugates by mixing and incubating a second set of antibodies (Ab2) with AuNPs in a buffered solution. Strong Ab2 adsorption to AuNPs proceeds through electrostatic, hydrophobic, and cysteine–gold interactions,[40] after which the AuNP–Ab2 conjugates are blocked by incubation in a bovine serum albumin (BSA) solution and cleaned via centrifugation (Scheme S1), generating monodisperse nanoparticles that can bind selectively to the antibody's antigen (Figure S1). We incubated the Ab1-modified surface with samples to capture the target molecule and then washed the surface with a BSA solution to block nonspecific binding. The solution of Ab2–AuNP conjugates is then incubated on the surface, generating an Ab1–PA_{83}–Ab2–AuNP sandwich structure. Incubation with a reducing agent (ascorbic acid) in a platinum salt solution selectively reduces Pt onto the nanoparticles, resulting in colorimetric detection with signal amplification. This process forms a Pt shell on the AuNPs, which catalyzes the splitting of hydrogen peroxide and subsequent oxidation of the chromogenic dye 3,3′,5,5′-tetramethylbenzidine (TMB) to yield a blue color that can be quantified on a plate reader.[33] To achieve scanometric detection, the Ab1–PA_{83}–Ab2–AuNP sandwich is generated on an NHS-activated glass slide. Incubation in a solution of Au^{3+} salt with a reducing agent (hydroxylamine) selectively reduces gold onto the nanoparticles. After washing, the light scattering from the gold on the slide is quantified in a Scano-miR instrument.

Screen for Anti-PA_{83} Monoclonal Antibody Sandwich.

To evaluate the scalability of the assay's colorimetric readout method, we screened monoclonal antibodies of anthrax protective antigen to discover pairs that could function in a sandwich assay. Because of PA_{83}'s role as an exotoxin protein expressed early during anthrax infections and because PA_{83} levels track levels of bacteremia in anthrax animal models,[41] PA_{83} has been used for years as a biomarker for the early detection of anthrax.[17,42–46] While many anti-PA_{83} monoclonal antibodies are commercially available and a few anti-PA_{83} monoclonal antibody sandwich pairs have been reported,[47] no sandwich pairs of

monoclonal antibodies for PA_{83} are commercially available, potentially limiting the long-term reproducibility of any given PA_{83} immunoassay.[48,49]

We addressed this by investigating 7 different anti-PA_{83} antibodies from Abcam (Ab8240, Ab1988, Ab1990, Ab1992, Ab13808, and Ab38725), immobilizing each of them in 8-well rows to form an 8 × 8 well array on an NHS-modified 96-well plate. After washing with a BSA blocking solution, all wells were incubated with 500 nM PA_{83} and washed with blocking solution again. We then incubated each 8-well row pairwise with 7 different mAb–AuNP conjugates to generate all possible Ab1–PA_{83}–Ab2–AuNP sandwiches. After washing again with blocking solution, a Pt salt solution was reduced onto the immobilized particles. We gently rinsed the wells with DI water, and then incubated them with TMB and 50 mM H_2O_2. One mAb pair, Ab8240 and Ab1992, gave a colorimetric and UV–vis absorbance signal that was 20-fold higher than the BSA control and 8-fold higher than any other antibody pair (Figures 1 and S2). Although the initial screen indicated that immobilized Ab8240– and Ab1992–AuNP generated a greater colorimetric signal than immobilized Ab1992– and Ab8240–AuNP, further experiments showed that both antibody pair orientations in the sandwich gave a similar detection sensitivity (Figure 2). To validate the obtained antibody pair, we tested them in a standard ELISA. #Ab1992 and #Ab8240 readily detected PA_{83} in an ELISA, while other antibody pairs either displayed no response above the background or only responded to higher PA_{83} concentrations (Figure S3).

Colorimetric PA_{83} Detection in Phosphate-Buffered Saline.

Having discovered an antibody pair with high selectivity for PA_{83}, we explored its ability to colorimetrically detect PA_{83} in PBS. Reaction conditions, including the H_2O_2 concentration (20–100 mM), Pt reduction time (10–120 min), and PA_{83} and mAb–AuNP incubation times (15–60 min), were varied to maximize the colorimetric response to PA_{83} and minimize the background signal (Figures S4–S6). Additionally, 1 h PA_{83} and mAb–AuNP incubation steps, a 120 min Pt reduction step, and 100 mM H_2O_2 concentrations in the TMB/H_2O_2 solution produced the largest response to the lowest [PA_{83}] relative to the background signal. The colorimetric readout provides the ability to detect PA_{83} over the 1 to 500 nM dynamic range (Figure 3 and S7), with a visual detection of 1 nM PA_{83} after a 20 min incubation and a colorimetric detection of 1 nM PA_{83} within 2 min of adding TMB in a plate reader.

PA_{83} Detection in Human Serum.

One of the primary advantages of sandwich assays is their ability to specifically detect analytes in a complex solution, like bodily fluids. Therefore, we tested the ability of the antibody pair to detect PA_{83} in human serum over the 0.5 to 100 nM range in 1:1 PBS:human serum samples (Figure 4). To determine the utility of the antibody sandwich, we attempted direct PA_{83} detection with a single mAb, by incubating PA_{83}-spiked serum samples in unblocked NHS-modified wells, before adding the mAb–AuNP conjugate. After a 20 min incubation in the colorimetric detection solution, the mAb sandwich displayed a dose response from 10 to 100 nM PA_{83}, while the single mAb failed to detect any PA_{83} concentration, thereby demonstrating the importance of the sandwich assay for detecting PA_{83} in complex, physiologically relevant solutions. In a blinded test of colorimetric PA_{83} detection in a 1:1 PBS:serum, we further improved the colorimetric detection of PA_{83} to 5

nM by allowing the final incubation in the colorimetric detection solution to run overnight. Because the serum is diluted 1:1 in PBS, these experiments demonstrate detection down to 10–20 nM PA_{83} (830–1660 ng/mL) in whole serum. This is within the physiological range of PA_{83} concentrations observed in the serum of rabbits (1–100,000 ng/mL) and guinea pigs (1–5000 ng/mL) during the progression of inhalational of anthrax.[50] However, the PA_{83} concentrations detected by this colorimetric assay correspond to more advanced stages of anthrax rather than the early, potentially treatable stage, at least in these two animal models, so more sensitive methods of signal amplification and detection are desirable to make an assay that could potentially enable early diagnosis and successful treatment of anthrax.

Scanometric Detection of PA_{83}.

Although the colorimetric mAb–AuNP sandwich was successfully used to screen for and discover an antibody sandwich pair that could detect pathogenically relevant concentrations of PA_{83}, assay sensitivity to even lower concentrations could potentially enable earlier diagnosis and successful treatment. This is particularly important for anthrax, as the expression of protective antigen facilitates the endocytosis of the lethal factor and edema factor toxins required for disease progression.[51,52] We therefore sought to determine whether measuring the scanometric readout of the sandwich immunoassay increased detection sensitivity (Figure 5). Ab1992 was functionalized on an NHS-activated glass slide and incubated first with PA_{83} and then with Ab8240–AuNP, with blocking steps in between. A gold reduction solution was added to the slide to amplify the gold signal. Scattering light of a 633 nm laser across the slide was collected in a Scano-miR instrument (Figure S8) and quantified with GenePix software. The scanometric assay detected PA_{83} at concentrations ranging from 600 fM to 60 nM in PBS with 1% BSA and 0.02% Tween, with a limit of detection of 550 fM. This is over 1000 times more sensitive than the Pt-based colorimetric assay of PA_{83} in the same solution. These results underscore the observation that the gold reduction and scanometric readout is a general strategy for increasing the sensitivity of antibody sandwich assays. This could be particularly useful for biomarkers of an infection such as PA_{83}, for which early identification of the pathogen can be critical for successfully treating the disease.[53]

CONCLUSION

The dual-readout sandwich immunoassay presented here enables both a device-free visual and colorimetric analysis of samples as well as highly sensitive scanometric target detection. Previous work on dual-readout Pt-coated AuNP detection strategies used the local surface plasmon resonance (LSPR) of AuNPs to detect them colorimetrically and therefore required the careful deposition of only a few layers of Pt atoms onto the AuNPs to avoid disrupting their LSPR.[37] In this approach, the Pt-based colorimetric readout is more sensitive than the Au-based colorimetric detection. By contrast, our assay demonstrates much greater sensitivity through the gold-based readout than the Pt-based one, highlighting the value of the gold amplification step and scanometric detection method. The subpicomolar scanometric readout's detection sensitivity is comparable to other ultrasensitive nanoparticle-based PA_{83} assays employing europium nanoparticle-based fluorescence and silver nanoparticle-enhanced fluorescence.[17,44]

One way to improve this assay would be to reduce the time required to get a colorimetric readout. This could be achieved by increasing the concentration of K_2PtCl_6 and shortening the incubation time during the platinum deposition step. The platinum metal precursor solution used in this work is based on prior research into the synthesis of colloidally stable Au@Pt nanostructures.[32] However, in our assay, the colloidal stability of the immobilized AuNPs after Pt deposition is unimportant; what matters is that Pt is specifically deposited only on the AuNPs.

Another approach to minimize time-to-readout could be to conjugate antibodies directly to peroxidase-mimicking nanoparticles,[54] which are capable of both catalytic H_2O_2 splitting and nucleation of gold particle growth from reduced ions. Gold nanoclusters (AuNCs), for instance, can catalyze the splitting of O_2 and subsequent oxidation of TMB when illuminated with visible light.[55] Alternatively, anisotropic platinum nanoparticles (PtNPs) can split H_2O_2 and oxidize TMB without a reduction step and have been functionalized with immunoglobulins to create model immunoassays.[16] If PtNPs could serve as nuclei for gold reduction then mAb–PtNPs could provide even more rapid device-free colorimetric antigen detection, while still enabling highly sensitive scanometric detection with the same particles.

The colorimetric detection readout developed in this work has a similar sensitivity to colorimetric immunoassays employing the enzyme horseradish peroxidase (e.g., ELISA). Another H_2O_2-decomposing enzyme, catalase, has been combined with gold NPs to achieve ultrasensitive visual detection of protein biomarkers.[57] However, in contrast to most enzymes, Pt remains catalytically active across a wide range of temperatures and pH's,[16] broadening the range of applications and potentially enhancing the field deployability of similar colorimetric assays. Although less sensitive than the scanometric readout, in principle, the colorimetric readout could be employed in pairwise device-free screens to discover pairs of recognition elements, such as antibodies, aptamers, or hyper-stable designer protein binders,[58] while the scanometric detection method can be used to significantly increase the sensitivity of any discovered sandwich pairs. These paired recognition elements, like the anti-PA_{83} mAb pair discovered using the colorimetric readout, could serve as practical tools for the sensitive, specific, and reproducible detection of anthrax and other disease biomarkers.

Supplementary Material

Refer to Web version on PubMed Central for supplementary material.

ACKNOWLEDGMENTS

This material is based on research sponsored by Air Force Research Laboratory agreement FA8650-15-2-5518; the Office of the Director of National Intelligence, Intelligence Advanced Research Projects Activity, via Federal Bureau of Investigation Contract DJF-15-1200-K-0001730; the Air Force Office of Scientific Research Awards FA9550-18-1-0493 and FA9550-16-1-0150; the NTU-NU Institute for NanoMedicine located at the International Institute for Nanotechnology, Northwestern University, US, and the Nanyang Technological University, Singapore; and the National Cancer Institute of the National Institutes of Health Awards U54CA199091 and U54CA151880. Research reported was also supported by the following training programs: The Cellular and Molecular Basis of Disease Training Program funded by the National Institutes of Health, Institute of General Medical Sciences Award T32GM008061, and the Chemistry of Life Processes Training Program in conjunction with National Institute of General Medical Sciences Award T32GM105538. The content is solely the responsibility of the authors and does not necessarily represent the official views of the sponsors or the US Government.

REFERENCES

(1). Speers DJ Clin. Biochem. Rev 2006, 27 (1), 39–51. [PubMed: 16886046]

(2). Slagle KM; Ghosn SJ Lab. Med 1996, 27, 177–183.

(3). Lequin RM Clin. Chem 2005, 51, 2415–2418. [PubMed: 16179424]

(4). Porstmann T; Kiessig ST J. Immunol. Methods 1992, 150, 5–21. [PubMed: 1613258]

(5). Tang S; Hewlett IJ Infect. Dis 2010, 201, S59–S64.

(6). Díez-Buitrago B; Briz N; Liz-Marzán LM; Pavlov V Analyst 2018, 143, 1727–1734. [PubMed: 29552682]

(7). Zheng A-X; Li J; Wang J-R; Song X-R; Chen G-N; Yang H-H Chem. Commun 2012, 48, 3112–3114.

(8). Farka Z; Juřík T; Kovář D; Trnková L; Skládal P Chem. Rev 2017, 117, 9973–10042. [PubMed: 28753280]

(9). Rosi NL; Mirkin CA Chem. Rev 2005, 105 (4), 1547–1562. [PubMed: 15826019]

(10). Kelley SO; Mirkin CA; Walt DR; Ismagilov RF; Toner M; Sargent EH Nat. Nanotechnol 2014, 9, 969–980. [PubMed: 25466541]

(11). El-Ansary A; Faddah LM Nanotechnol., Sci. Appl 2010, 3, 65–76. [PubMed: 24198472]

(12). Elghanian R; Storhoff JJ; Mucic RC; Letsinger RL; Mirkin CA Science 1997, 277, 1078–1081. [PubMed: 9262471]

(13). Storhoff JJ; Elghanian R; Mucic R; Mirkin CA; Letsinger RL J. Am. Chem. Soc 1998, 120, 1959–1964.

(14). Lee J-S; Ulmann PA; Han MS; Mirkin CA Nano Lett. 2008, 8, 529–533. [PubMed: 18205426]

(15). Ambrosi A; Airò F; Merkoçi A Anal. Chem 2010, 82, 1151–1156. [PubMed: 20043655]

(16). Gao Z; Xu M; Hou L; Chen G; Tang D Anal. Chim. Acta 2013, 776, 79–86. [PubMed: 23601285]

(17). Tang S; Moayeri M; Chen Z; Harma H; Zhao J; Hu H; Purcell RH; Leppla SH; Hewlett IK Clin. Vaccine Immunol 2009, 16 (3), 408–413. [PubMed: 19129473]

(18). Chinen AB; Guan CM; Ferrer JR; Barnaby SN; Merkel TJ; Mirkin CA Chem. Rev 2015, 115, 10530–10574. [PubMed: 26313138]

(19). Geißler D; Charbonnière LJ; Ziessel RF; Butlin NG; Löhmannsröben H-G; Hildebrandt N Angew. Chem., Int. Ed 2010, 49, 1396–1401.

(20). Bilan R; Ametzazurra A; Brazhnik K; Escorza S; Fernandez D; Uribarri M; Nabiev I; Sukhanova A Sci. Rep 2017, 7 (1), 44668. [PubMed: 28300171]

(21). Prigodich AE; Randeria PS; Briley WE; Kim NJ; Daniel WL; Giljohann DA; Mirkin CA Anal. Chem 2012, 84, 2062–2066. [PubMed: 22288418]

(22). Halo TL; McMahon KM; Angeloni NL; Xu Y; Wang W; Chinen AB; Malin D; Strekalova E; Cryns VL; Cheng C; Mirkin CA; Thaxton CS Proc. Natl. Acad. Sci. U. S. A 2014, 111, 17104–17109. [PubMed: 25404304]

(23). Zheng D; Seferos DS; Giljohann DA; Patel PC; Mirkin CA Nano Lett. 2009, 9, 3258–3261. [PubMed: 19645478]

(24). Alhasan AH; Scott AW; Wu JJ; Feng G; Meeks JJ; Thaxton CS; Mirkin CA Proc. Natl. Acad. Sci. U. S. A 2016, 113, 10655–10660. [PubMed: 27601638]

(25). Kim D; Daniel WL; Mirkin CA Anal. Chem 2009, 81, 9183–9187. [PubMed: 19874062]

(26). Scott AW; Garimella V; Calabrese CM; Mirkin CA Bioconjugate Chem. 2017, 28, 203–211.

(27). Tian D; Duan C; Wang W; Cui H Biosens. Bioelectron 2010, 25, 2290–2295. [PubMed: 20392629]

(28). Arya SK; Estrela P Sensors 2018, 18, 2010.

(29). Ashley MJ; Bourgeois MR; Murthy RR; Laramy CR; Ross MB; Naik RR; Schatz GC; Mirkin CA J. Phys. Chem. C 2018, 122, 2307–2314.

(30). Zhang K; Wang Y; Wu M; Liu Y; Shi D; Liu B Chem. Sci 2018, 9, 8089–8093. [PubMed: 30542557]

(31). Li Y; Lu Q; Wu S; Wang L; Shi X Biosens. Bioelectron 2013, 41, 576–581. [PubMed: 23062554]

(32). Roy RK; Njagi JI; Farrell B; Halaciuga I; Lopez M; Goia DV J. Colloid Interface Sci 2012, 369, 91–95. [PubMed: 22197295]

(33). He W; et al. Biomaterials 2011, 32, 1139–1147. [PubMed: 21071085]

(34). Nam J-M; Thaxton CS; Mirkin CA Science 2003, 301, 1884–1886. [PubMed: 14512622]

(35). Hill HD; Mirkin CA Nat. Protoc 2006, 1, 324–336. [PubMed: 17406253]

(36). Zhao J; Wang S; Lu S; Liu G; Sun J; Yang X Anal. Chem 2019, 91, 7828–7834. [PubMed: 31124658]

(37). Gao Z; Ye H; Tang D; Tao J; Habibi S; Minerick A; Tang D; Xia X Nano Lett. 2017, 17, 5572–5579. [PubMed: 28813601]

(38). Zhang R; Li N; Sun J; Gao FJ Agric. Food Chem 2015, 63, 8947–8954.

(39). Frens G Nature, Phys. Sci 1973, 241, 20–22.

(40). Jazayeri MH; Amani H; Pourfatollah AA; Pazoki-Toroudi H; Sedighimoghaddam B Sens. Bio-Sensing Res 2016, 9, 17–22.

(41). Kobiler D; Weiss S; Levy H; Fisher M; Mechaly A; Pass A; Altboum Z Infect. Immun 2006, 74, 5871–5876. [PubMed: 16988266]

(42). Mabry R; Brasky K; Geiger R; Carrion R Jr.; Hubbard GB ; Leppla S; Patterson JL; Georgiou G; Iverson BL Clin. Vaccine Immunol 2006, 13, 671–677. [PubMed: 16760326]

(43). Morel N; Volland H; Dano J; Lamourette P; Sylvestre P; Mock M; Creminon C Appl. Environ. Microbiol 2012, 78, 6491–6498. [PubMed: 22773632]

(44). Dragan AI; Albrecht MT; Pavlovic R; Keane-Myers AM; Geddes CD Anal. Biochem 2012, 425, 54–61. [PubMed: 22406431]

(45). Ghosh N; Gupta N; Gupta G; Boopathi M; Pal V; Goel AK Diagn. Microbiol. Infect. Dis 2013, 77, 14–19. [PubMed: 23773677]

(46). Oh BN; Lee S; Park HY; Baeg JO; Yoon MY; Kim J Analyst 2011, 136, 3384–3388. [PubMed: 21743920]

(47). Rudenko NV; Abbasova SG; Grishin EV Bioorg. Khim 2011, 37 (3), 354–360. [PubMed: 21899050]

(48). Siddiqui MZ Indian J. Pharm. Sci 2010, 72, 12–17. [PubMed: 20582184]

(49). Hanly WC; Artwohl JE; Bennett BT ILAR J. 1995, 37, 93–118. [PubMed: 11528030]

(50). Savransky V; et al. Infect. Immun 2013, 81, 1152–1163. [PubMed: 23357384]

(51). Kintzer AF; Thoren KL; Sterling HJ; Dong KC; Feld GK; Tang II; Zhang TT; Williams ER; Berger JM; Krantz BA J. Mol. Biol 2009, 392, 614–629. [PubMed: 19627991]

(52). Singh Y; Klimpel KR; Goel S; Swain PK; Leppla SH Infect. Immun 1999, 67, 1853–1859. [PubMed: 10085027]

(53). Kamal SM; Rashid AKMM; Bakar MA; Ahad MA Asian Pac. J. Trop. Biomed 2011, 1, 496–501. [PubMed: 23569822]

(54). Huang Y; Ren J; Qu X Chem. Rev 2019, 119, 4357–4412. [PubMed: 30801188]

(55). Wang G-L; Jin L-Y; Dong Y-M; Wu X-M; Li Z-J Biosens. Bioelectron 2015, 64, 523–529. [PubMed: 25310483]

(56). Moayeri M; Wiggins JF; Leppla SH Infect. Immun 2007, 75, 5175–5184. [PubMed: 17724066]

(57). de la Rica R; Stevens MM Nat. Nanotechnol 2012, 7, 821–824. [PubMed: 23103935]

(58). Chevalier A; et al. Nature 2017, 550, 74–79. [PubMed: 28953867]

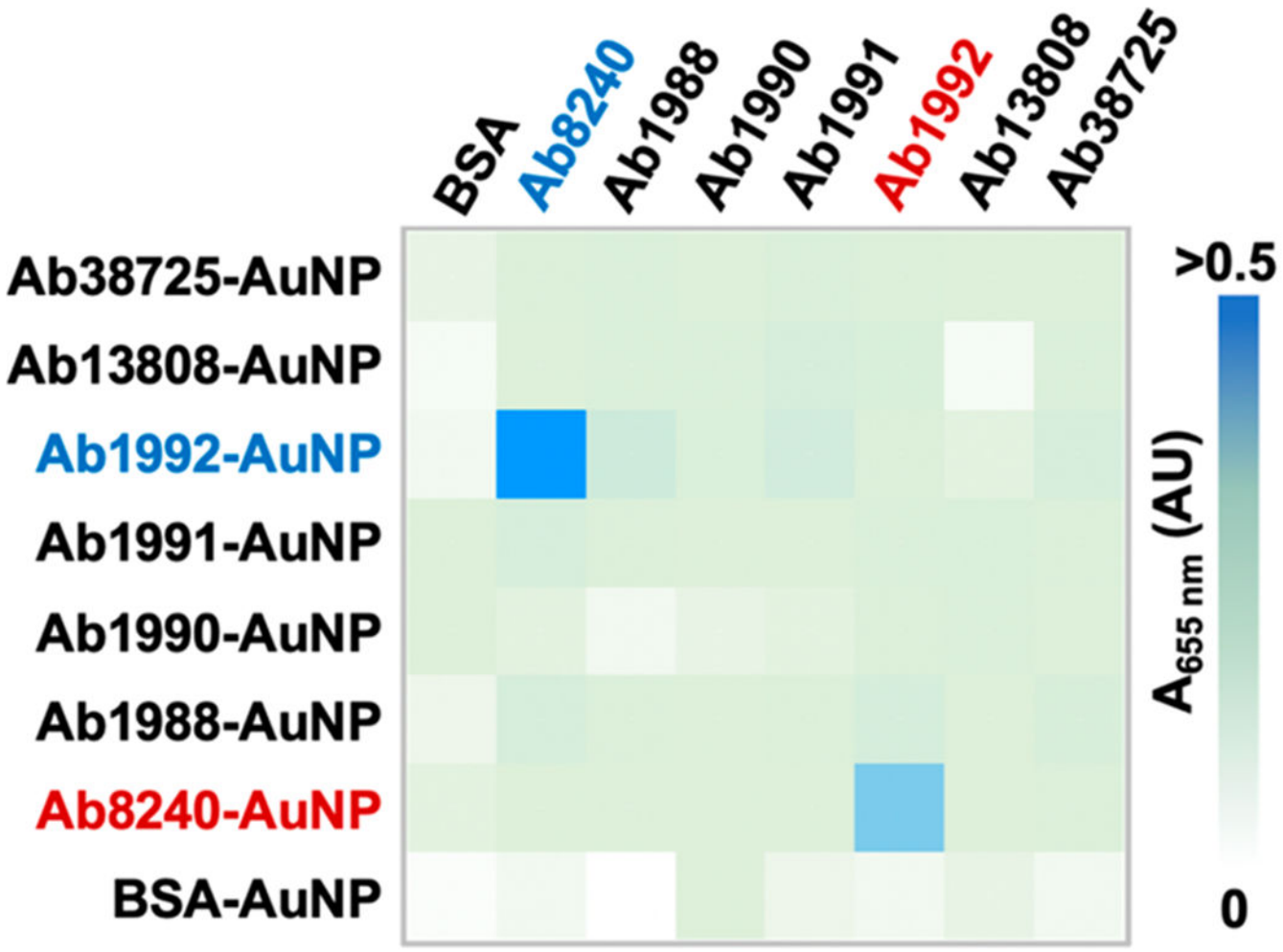

Figure 1.

Heatmap of a pairwise screen of seven commercial anti-PA_{83} antibodies for binding and detection of PA_{83} in a sandwich assay. Each column contains a different Ab immobilized in the well, while each row is incubated with a different mAb–AuNP nanoparticle. Ab1992 and Ab8240 form a sandwich pair and detect PA_{83} in both orientations (blue and red).

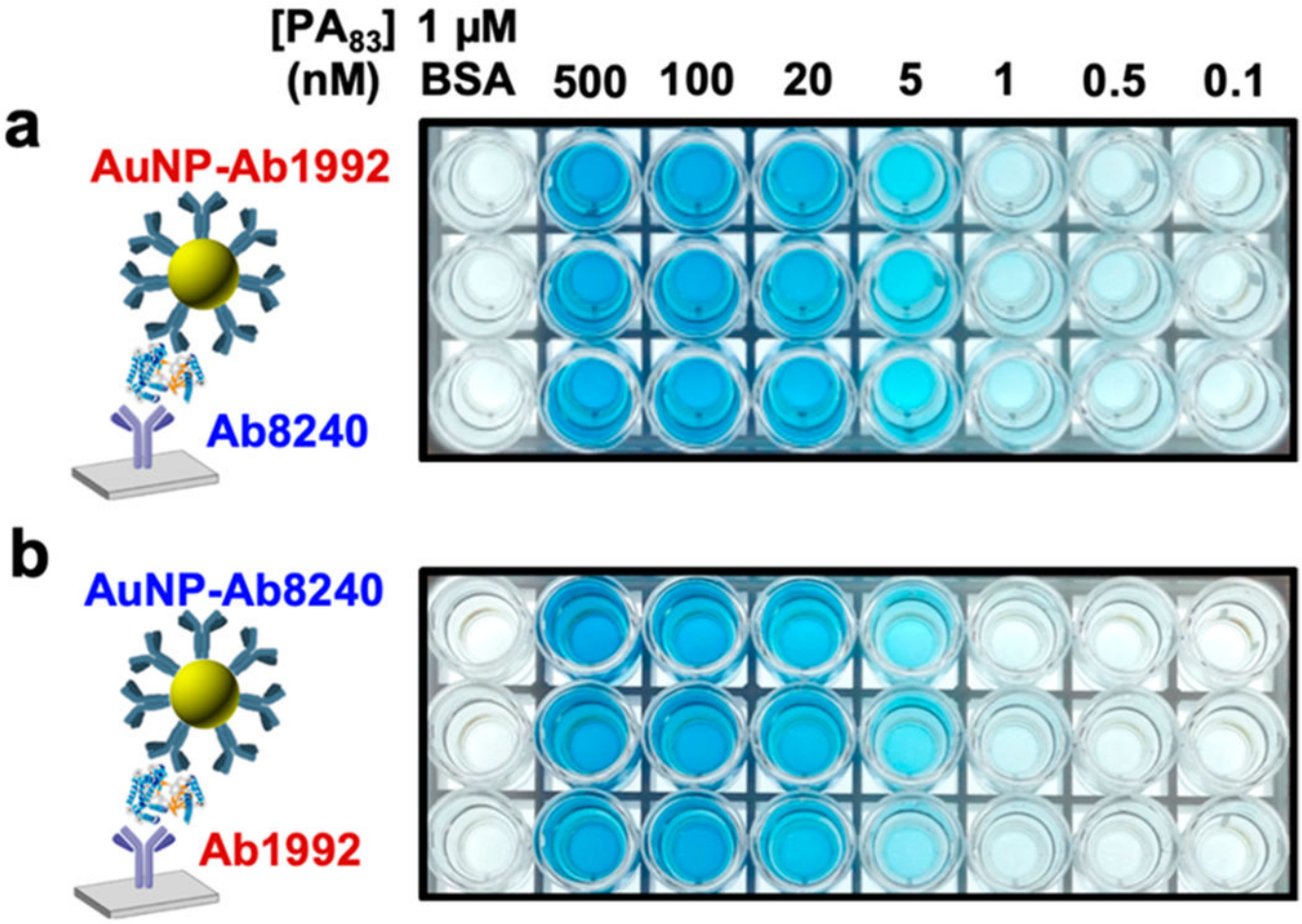

Figure 2.

Sandwich assay performs device-free PA_{83} detection in either antibody orientation. (a) Detection of PA_{83} in PBS with immobilized Ab1992– and Ab8240–AuNP. (b) Detection of PA_{83} in PBS with immobilized Ab8240– and Ab1992–AuNP.

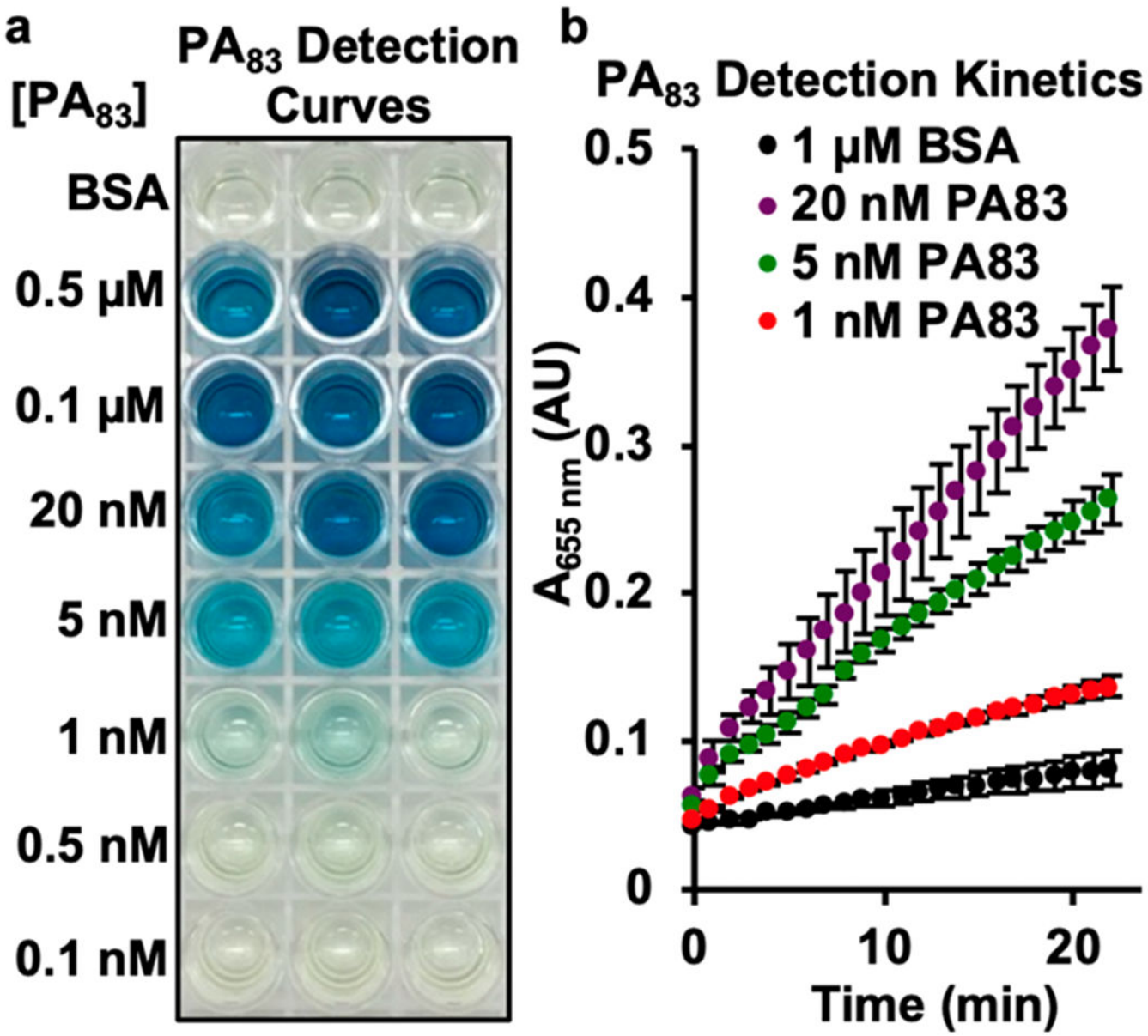

Figure 3.

Visual and colorimetric detection of PA_{83}. (a) Triplicate visual detection of PA_{83} after 1 h of Pt reduction and 20 min of TMB/H_2O_2 reaction. Control condition: 1 μM BSA. (b) Kinetics of PA_{83} detection with TMB/H_2O_2.

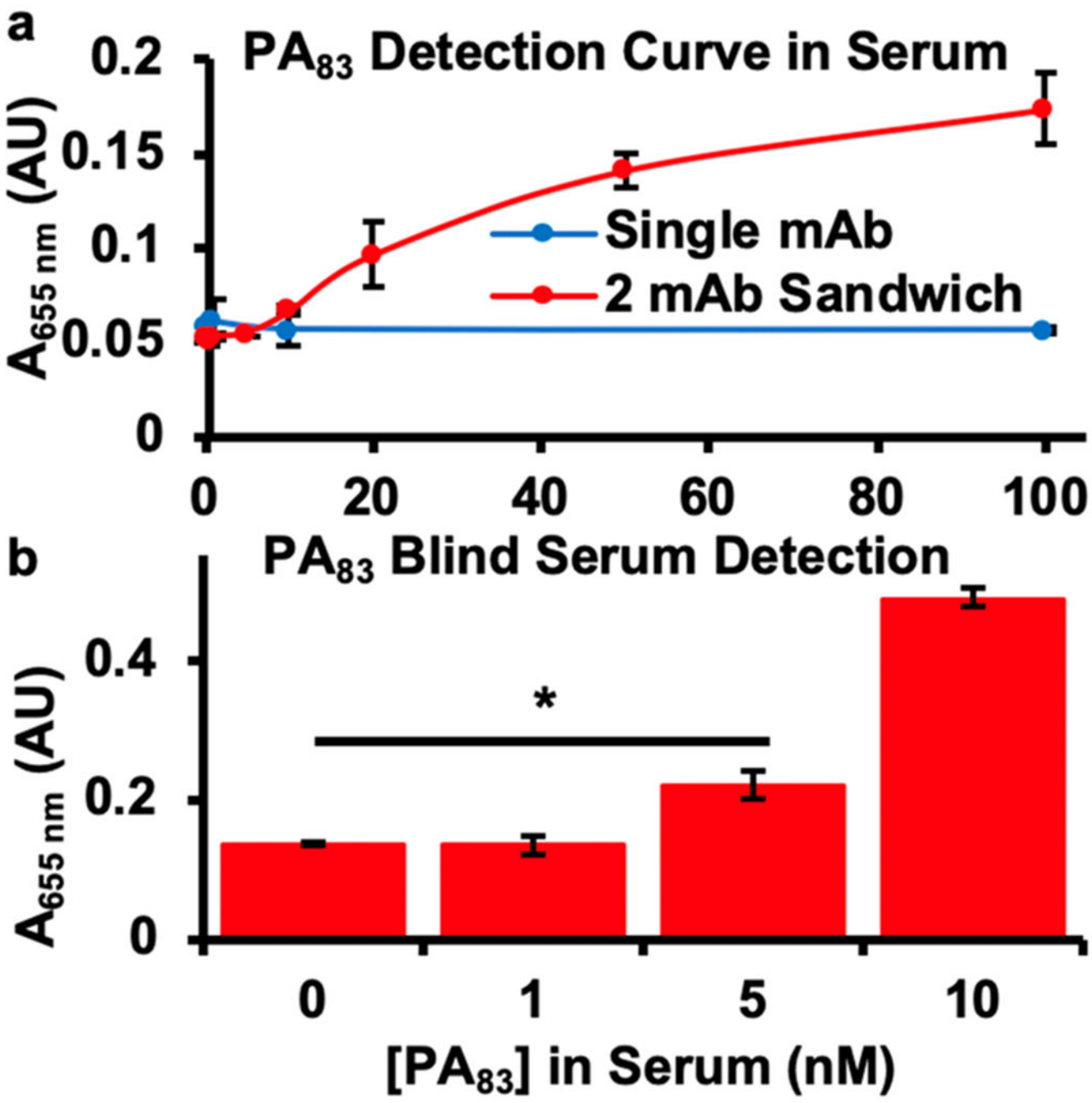

Figure 4.

Detection of PA_{83} in serum. (a) Detection of PA_{83} spiked into 1:1 PBS:human serum with a single Ab (blue) and with the sandwich mAb pair (red). (b) Blind detection of nanomolar PA_{83} in human serum. (*$p < 0.01$, Student's *t*-test).

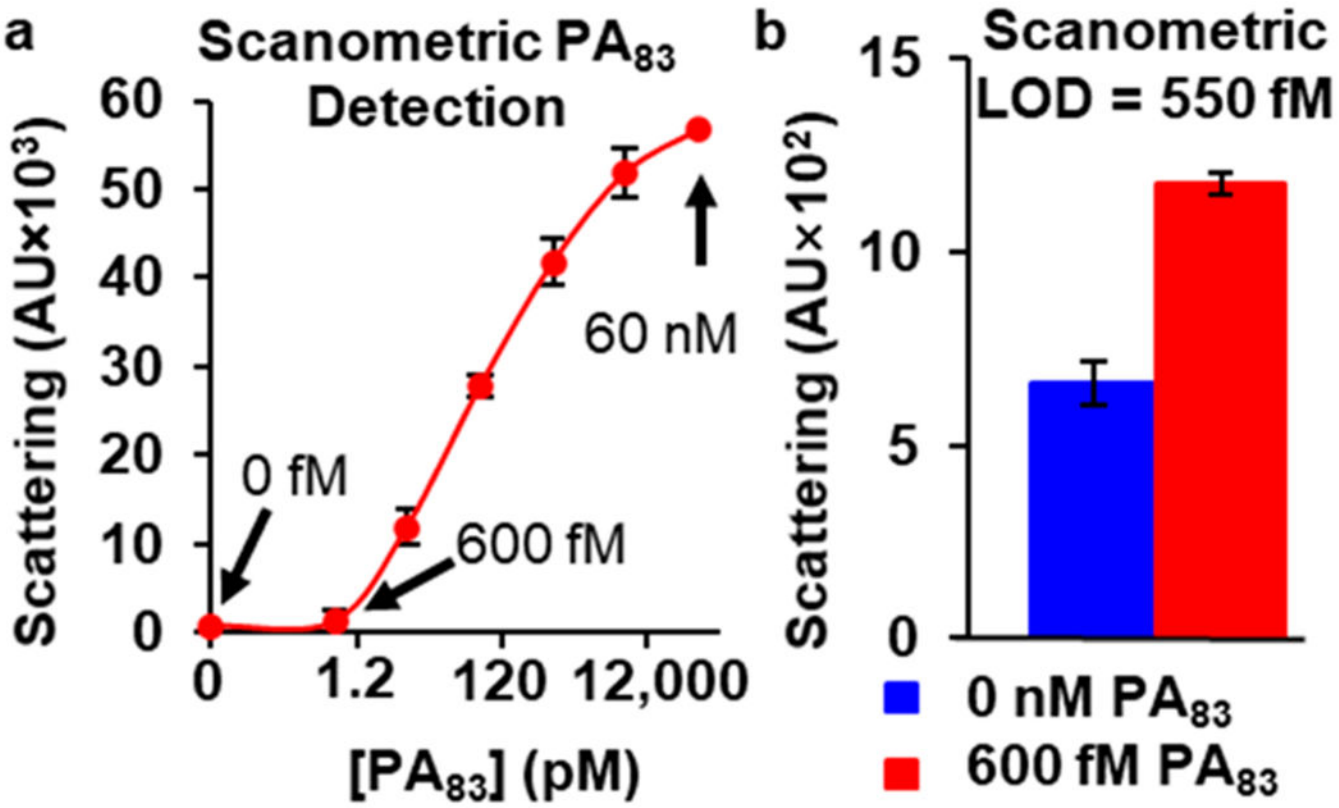

Figure 5.

Scanometric detection of PA_{83} via gold reduction onto mAb–AuNP sandwich. (a) Quantification of scanometric PA_{83} detection using 633 nm light scattering. (b) Detection of subpicomolar concentrations of PA_{83}.

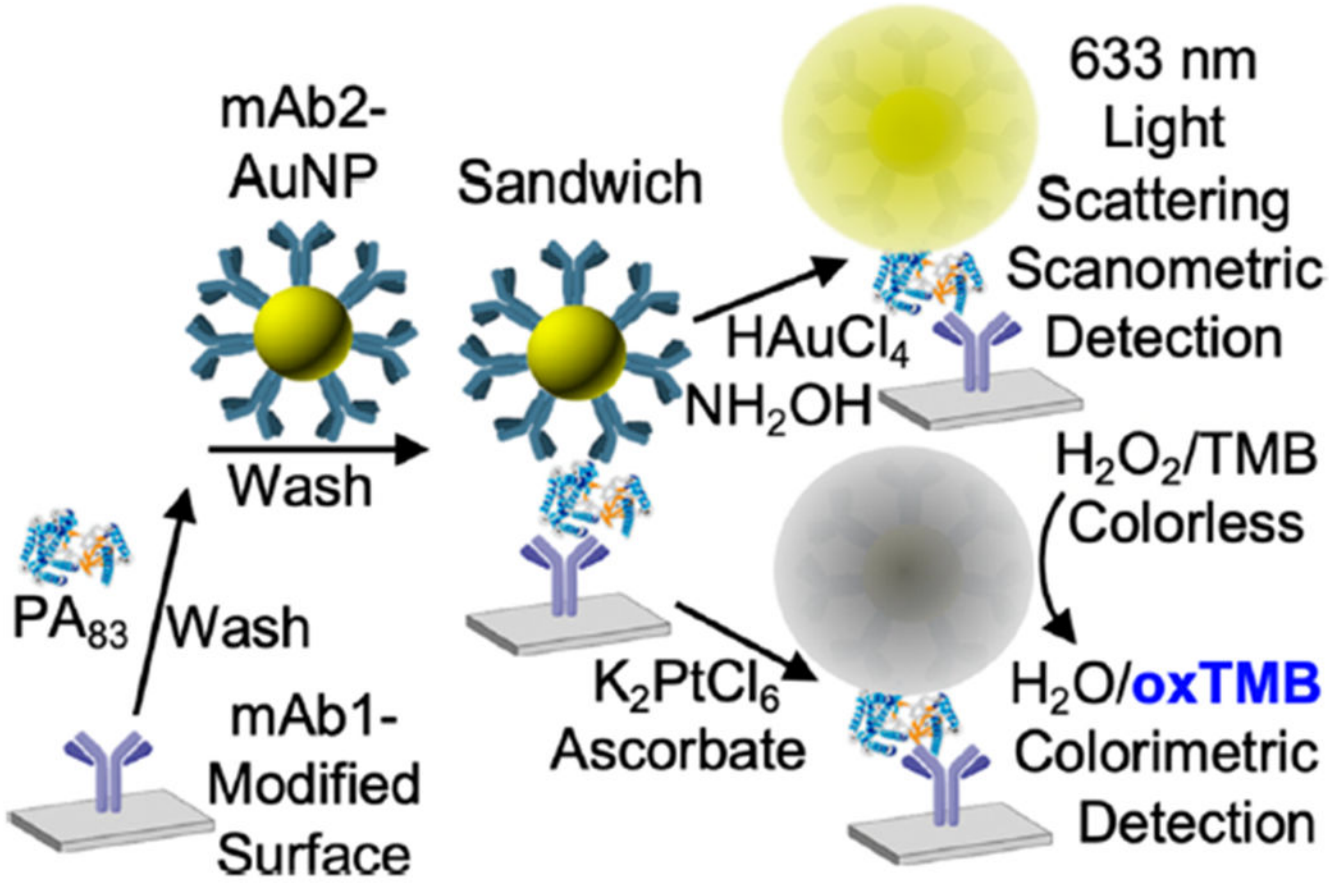

Scheme 1.
Dual-Readout AuNP-Based Immunoassay to Detect Anthrax Protective Antigen